Final Draft
of the original manuscript:

Maawad, E.; Brokmeier, H.-G.; Hofmann, M.; Genzel, C.; Wagner, L.:
Stress distribution in mechanically surface treated Ti-2.5Cu determined by combining energy-dispersive synchrotron and neutron diffraction
In: Materials Science and Engineering A (2010) Elsevier

DOI: 10.1016/j.msea.2010.05.044

Stress distribution in mechanically surface treated Ti-2.5Cu determined by combining energy-dispersive synchrotron and neutron diffraction

E. Maawad [a],*, H.-G. Brokmeier [a,b], M. Hofmann [c], Ch. Genzel [d], L. Wagner [a]

[a] Institute of Materials Science and Engineering, Clausthal University of Technology, Clausthal-Zellerfeld, Germany

[b] Institute of Materials Research, GKSS Research Center, Geesthacht, Germany

[c] Forschungsneutronenquelle Heinz Maier-Leibnitz (FRM-II), TU München, Germany

[d] Helmholtz-Zentrum Berlin (BESSY), Berlin, Germany

Abstract

Mechanical surface treatments such as shot peening (SP) or ball-burnishing (BB) induce plastic deformation close to the surface resulting in work-hardening and compressive residual stresses. It enhances the fatigue performance by retarding or even suppressing micro-crack growth from the surface into the interior. SP and BB were carried out on a solution heat treated (SHT) Ti-2.5Cu. The investigations of compressive and balancing tensile residual stresses need a combination of energy-dispersive synchrotron (ED) and neutron diffraction. Essential for the stress distribution is the stress state before surface treatments which was determined by neutron diffraction.

Results show that the maximum compressive stress and its depth play an important role to improve the fatigue performance.

Keywords: shot peening; ball-burnishing; residual stress; synchrotron radiation; neutron diffraction; Ti-2.5Cu

---

* Corresponding author. Tel.: +49-05323-72-2758; fax: +49-05323-72-2766.
E-mail address: emad.k.s.maawad@tu-clausthal.de
Postal address: IWW, Agricolastr. 6, 38678 Clausthal-Zellerfeld, Germany.

1. Introduction

The beneficial influence of mechanical surface treatments on the high cycle fatigue (HCF) performance of engineering components is often explained by induced high dislocation densities and compressive residual stresses. This is attributed to the induced plastic deformation produced by the kinetic energy of the shots during shot peening (SP) process or by the ball pressure during ball-burnishing (BB) process, which results in work-hardening and generation of residual stresses. Some studies have been carried out to investigate the influence of mechanical surface treatments on the fatigue performance of Ti-2.5Cu. It was found that the fatigue endurance stresses was improved by 45% after SP [1-3] and 60 % after BB [3] in rotating beam loading (R = -1). Such improvements have revealed that the failure is associated with subsurface fatigue crack nucleation. This phenomenon may be related to the presence of a process-induced tensile residual stress necessarily present below the mechanically treated surface and required to balance compressive residual stress induced by the surface treatment process [4]. This balancing tensile residual stresses could be either of the following two forms: firstly in a constant form (full line in Fig. 1) as described in the core region of a thin shot peened AISI 4140 steel plates [5]; secondly in a concentrated form (dashed line in Fig. 1) as found in a relatively thin layer after shot peening, laser shock peening or ultrasonic shot peening in 304 austenitic stainless steel [6]. Neutron diffraction is efficient in identification of the residual stresses in a variety of engineering materials which have experienced different shot peening treatments [7]. It was concluded that these stresses show surface compression balanced by subsurface tension of about one third of the surface compressive stress value. Furthermore, because of the finite volume of material needed for neutron measurements, it is difficult to produce precise

measurements within the first 100 μm from the surface. Consequently, laboratory X-rays (XRD) and energy dispersive synchrotron diffraction (ED) are used for depth profile of a few hundred μm to overcome the limitation of neutron diffraction [8-10]. ED and XRD were used to determine the residual stress depth distribution in shot peened Ti-2.5Cu with Almen intensities of 0.11 mmA and 0.20 mmA [11]. It was found that the maximum compressive residual stresses determined by XRD are higher than that by ED. This is attributed to the different spatial resolutions and corresponding gauge volumes. In addition, the residual stress-depth distribution obtained by ED is flatter than that by XRD. This is interpreted by the *'modified multi wavelength method'*, which yields to the residual stress depth distribution in the Laplace space, i.e. sigma (τ) which is explained elsewhere [13].

The main aim of the present study is to determine:

- residual stress distribution after SP or BB in some hundred micrometers from the surface by ED, and
- balancing tensile residual stress distribution by neutron diffraction.

The pre-residual stress induced due to both rolling process and solution heat treatment has to be taken into account.

2. Experiment

The Ti-2.5Cu alloy was received as 10 mm thick hot rolled plate. From this plate, quadratic samples (20 x 20 x 10 mm^3) were cut perpendicular to the rolling direction. The conventional equiaxed microstructure was achieved by solution heat treating (SHT) at 805°C for 1 hr followed by water-quenching. The microstructure of Ti-2.5Cu consists of α grains and stringers of the eutectoid component α + Ti_2Cu as shown in Fig. 2.

Threaded cylindrical tensile samples were machined having gauge length and diameter of 25 mm and 5 mm, respectively. Tensile properties of Ti-2.5Cu are listed in Table 1. The relatively lower yield strength and higher ductility result in a good formability. Therefore, Ti-2.5Cu is used in many applications including sheets, forgings and extrusions for fabricating components such as bypass ducts of gas-turbine engines as well as airframe industry.

Shot peening was performed using cast steel (S330) having a hardness of 460 HV and an average shot diameter of 0.80 mm. All peening was performed to full coverage using Almen intensity of 0.20 mmA. For comparison, Ti-2.5Cu samples were ball-burnished using a conventional lathe and a hydrostatic tool by which a hard metal ball (Ø6 mm) is pressed with pressure of 300 bar onto the sample surface.

Surface and near-surface characteristics were determined after SP or BB such as surface roughness, hardness and residual stress. Surface roughness was determined by means of an electronic contact (stylus) profilometer instrument. Microhardness HV0.1 was determined by using a Struers Duramin tester with a force of 100 ponds and a loading time of 10 seconds. Three measurements were taken at each depth to construct the hardness-depth distribution. In addition, residual stress depth distribution was determined using both ED and neutron diffraction.

2.1 Energy Dispersive Synchrotron Diffraction (ED)

Residual stress measurements were performed by hard x-ray diffraction using synchrotron radiation at BESSY-II in Berlin. The characteristic of the used beamline EDDI offers a white X-ray beam with an energy range of 10 ~ 120 keV. The primary beam cross-section was defined by 0.5 x 0.5 mm^2, the angular divergence in the diffracted beam was restricted

by a double slit system with apertures of 0.03 x 5 mm^2 to $\Delta\theta \leq 0.005°$. To achieve a high information depth which depends on the absorption of the material, a scattering angle $2\theta = 8°$ was chosen. ED gives complete diffraction spectra for a fixed detector position. Any Bragg reflection was obtained by a different X-ray energy (wavelength) which means the signal of any reflection belongs to a different depth in the sample as schematically shown in Fig. 3. Due to the restriction of the penetration power even by 120 keV sufficient results were obtained up to 100 µm. In order to get a stress distribution in deeper region, 5 samples were prepared. Layer removal by electro-polishing in steps of 100 µm or 150 µm allows determining depth distribution up to 500 µm. Furthermore, the measured residual stress values were corrected using the equation which is described elsewhere [12]. Residual stresses were evaluated by means of the $\sin^2\psi$ method in steps of $\Delta\psi = 4°$ up to 80°. A modified multi-wavelength approach [13] for any energy line $E_{(hkl)}$ gives an average penetration depth $\tau_{(hkl)}$ (Eq. 1).

$$\tau_{(hkl)} = (\tau_{(hkl)\,min} + \tau_{(hkl)\,max})/2 \qquad (1)$$

Where $\tau_{(hkl)min}$ and $\tau_{(hkl)\ max}$ are the minimum and the maximum penetration depths corresponding to the maximum and minimum tilting angles, respectively. The diffraction elastic constants of alpha - reflections in Ti-2.5Cu were calculated by the Kroener-Model [14].

2.2 Neutron Diffraction

Residual strains in the bulk of the material were determined using the neutron diffractometer (Stress-Spec) at FRM-II in Munich [15]. The measurement set-up is shown schematically in Fig. 4. As seen in Fig. 4, the gauge volume is defined by the dimension of both primary slit in the incident beam and secondary slit in the diffracted beam. The

parameters of the neutron diffractometer are listed in Table 2. As shown in Table 2, the size of the primary slit is 1 x 10 mm^2 and the secondary slit was opened with 1 mm in width. Therefore, the sampling gauge volume is a nearly square base of 1 x 1 mm^2 and a length of 10 mm. Because of the texture influences, the reflection (21.1) was used to determine the strain component within the surface plane (x-direction which is parallel to the rolling direction RD), while the (11.4) reflection was used to determine the strain component normal to the surface (z-direction). As the gauge volume is a relatively large with a spatial resolution of 500 μm and close to the surface, the partial filling of the gauge volume results in an artificial peak shift [16], it is difficult to precisely determine the stain distributions within 500 μm in depth. In that case, ED was used instead of neutrons to precisely determine the stain distributions within the first 500 μm from the mechanically treated surface. The values of the unstrained lattice parameter (d_o) were obtained from measurements of unpeened samples. Pre-strain distributions are found in these samples, and they are supposed to be caused by both the rolling process and the fast cooling rate through water quenching.

3. Results and Discussions

3.1 Microhardness

The microhardness-depth distribution of Ti-2.5Cu after SP and BB is shown in Fig. 5. It is clearly shown that maximum values at the surface after both surface treatments followed by a gradual decrease in hardness towards the interior. The bulk hardness value is about 250 HV0.1, while the hardness values at the surface are about 365 HV0.1 and 320 HV0.1 after SP and BB, respectively. Obviously, BB leads to much greater depths of plastic

deformation. The depth of induced plastic deformation is about 250 and 450 μm after SP and BB, respectively.

3.2 Surface roughness

The surface roughness after SP or BB was determined and compared to the electropolished (EP) sample as a reference. As seen in Fig. 6, the surface roughness of shot peened Ti-2.5Cu is much higher than that of the electropolished reference, while a remarkable improvement on the surface roughness is observed after BB. Apparently, the range of the surface roughness values is from 0.30 μm (EP) to 5.40 μm (SP), while the penetration depth (τ) of the first reflection (10.0) using ED is 14.17 μm. Therefore, the surface roughness influence can be ignored.

3.3 Residual stresses

The residual stress-depth distribution in Ti-2.5Cu after SP (Fig. 7-a) and BB (Fig. 7-b) was determined by combining ED and neutron diffraction. Obviously, the in-plane residual stress distributions (σ_{xx} // rolling direction RD) after SP or BB are different. While the residual stress normal to the surface ($\sigma_{zz} \perp$ RD) is constant within the depth and their values are 0 MPa and 50 MPa in shot peened and ball-burnished samples, respectively. This is explained by means of a radial material flow after SP or BB inducing only σxx and/or σ_{yy}. However it was found a small value of σ_{zz} after BB. This could be explained by a relatively higher hydrostatic pressure of 300 bar normal to the surface.

The most interested residual stress (σ_{xx}) values and their depths (τ) as well as corresponding improvements of the high cycle fatigue strength (HCF) [3] are compared and summarized in Table 3. Apparently, the maximum residual stress in shot peened Ti-2.5Cu (-687 MPa) is lower than that after BB (-750 MPa). This is due to BB leads to much greater depths of

plastic deformation as shown in the microhardness depth distribution (Fig. 5). Which means that the material tries to restore a highly plastic deformed original shape producing a cold worked material with high compressive stresses. Furthermore, contrary to what is expected, the zero-crossing depth is about 3 mm after SP and 1.5 mm after BB. This is explained by the influence of existing pre-stress with a zero-crossing depth of 3mm (Fig. 8). The much higher compressive residual stress after BB close to the surface overcomes the existing pre-stress and the zero-crossing depth shifts from 3mm to 1.5mm to get the balancing tensile stress.

As previously mentioned, the fatigue endurance stresses of Ti-2.5Cu are improved after SP or BB. This is a result of the induced-compressive residual stress. In the present study, it is observed that the maximum compressive residual stress and its depth play an important role to improve the HCF performance rather than the zero-crossing depth because it significantly retards the fatigue micro-cracks propagation. Furthermore, the balancing tensile residual stress is about 100 MPa and 50 MPa after SP and BB, respectively. It may be argued that the observed transition in fatigue crack nucleation site from surface to subsurface in mechanically surface treated conditions results from the presence of a high tensile residual stress at a location below the specimen surface [1]. As a result, the fatigue performance is also improved in BB samples compared to SP material.

5. Conclusions

Residual stress-depth distribution of mechanically surface treated Ti-2.5Cu (SHT) is investigated using both energy-dispersive synchrotron and neutron diffraction to determine the residual stress within 6 mm from the surface. It was found that zero-crossing depth is

about 3 and 1.5 mm in shot peened (SP) and ball-burnished (BB) samples, respectively. This is thought to be caused mainly by the influence of pre-stress. Moreover, the balanced tensile residual stress is constant in the thickness direction in the order of 100 MPa and 50 MPa after SP and BB, respectively. Maximum compressive residual stress and its depth are more significant to enhance fatigue life than the zero-crossing depth because it significantly retards fatigue cracks propagation. In addition, tensile residual stress could play an important role for a dramatic fatigue cracks nucleation and propagation.

Acknowledgements

The authors are indebted to the German Research Foundation (DFG) for financial support through BR961/5-1 and WA 692/32-1. This work was additionally supported by the European Community - Research Infrastructure Action under the FP6 "Structuring the European Research Area" Programme (through the Integrated Infrastructure Initiative" Integrating Activity on Synchrotron and Free Electron Laser Science - Contract R II 3-CT2004-506008)". The authors would also like to thank Dr. M. Klaus for assistance in the Synchrotron measurements.

Reference

[1] T. Ludian, M. Kocan, H. J. Rack, L. Wagner, J. Mat. Res. 97 (2006) 1425-1431.
[2] L. Wagner, M. Wollman, in: Proc. of the 10th Int. Conference on Shot Peening, K. Tosha (Eds.), Tokyo, Japan, 2008, pp. 355-362.
[3] T. Ludian, J. Atoura, L. Wagner, in: Proc. of the 10th Int. Conference on Shot Peening, edited by K. Tosha, Tokyo, Japan, 2008, pp. 375-380.
[4] E. Maawad, S. Yi, H.-G. Brokmeier, L. Wagner, in: Proc. of the 10th Int. Conference on Shot Peening, by K. Tosha, Tokyo, Japan, 2008, pp. 499-504.
[5] R. Menig, L. Pintschovius, V. Schulze, O. Voehringer, Scr. Mater. 45 (2001) 977-983.

[6] S. Clitheroe, M. Turski, A. Evans, J. Kelleher, D. Hughes, P. Withers, in: Proc. Of the 10th Int. Conference on Shot Peening, K. Tosha (Eds.), Tokyo, Japan, 2008, pp. 47-50.
[7] A. N. Ezeilo, G. A. Webster, P. S. Webster, L. Castex, in: Proc. of the 5th Int. Conference of Residual Stresses, T. Ericsson, M. Oden and A. Andersson (Eds.), Inst. of Tech., Linkopings Universitet, Sweden, 1997, pp. 726-731.
[8] F. Rotundo, A. M. Korsunsky, Procedia Engineering, 1 (2009) 221-224.
[9] M.N. Jamesa, D.J. Hughesb, Z. Chenb, H. Lombardc, D.G. Hattinghc, D. Asquithd, J.R. Yatesd, P.J. Webstere, Engineering Fail. Anal. 14 (2007) 384-395
[10] A. Pyzalla: Phys. B 276-278 (2000) 833-836.
[11] E. Maawad, H.-G. Brokmeier, L. Wagner, Ch. Genzel, in: Proc. of the 9th Int.Conference on Prod. Engineering, Des. and Control, M. El-Hofy (Eds.), Alexandria, Egypt, 2009, e-paper code 135.
[12] M.G. Moore, W.P. Evans, SAE Trans., 66 (1958) 340-345.
[13] Ch. Genzel, C. Stock, B. Wallis and W. Reimers: J. Nucl. Instrum. Methods A 467-468 (2001) 1253-1256.
[14] E. Kroener, Z. Phys. 151 (1958) 504-518.
[15] M. Hofmann, R. Schneider, G.A. Seidl, J. Rebelo-Kronmeier, R.C. Wimpory, U. Garbe, H.-G. Brokmeier, Phys. B, 385-386 (2006) 1035-1037.
[16] T. Keller, N. Margadant, T. Pirling, M.J. Riegert-Escribano, W. Wagner, Mater. Sci. And Engineering A 373 (2004) 33-44.

Figure Captions

Figure 1. Schematic presentation of the residual-stress distribution which might be expected after mechanical treatments, xo denotes the zero-crossing depth [5]
Figure 2. Microstructure of the Ti-2.5Cu alloy (SHT), average grain size ≈ 20 μm
Figure 3. Scheme showing a relation between energy and penetration depth
Figure 4. Schematic set-up of the neutron scattering experiment at FRM-II
Figure 5. Microhardness depth-distribution of Ti-2.5Cu after SP and BB
Figure 6. Roughness values of the various surface treated conditions in Ti-2.5Cu (EP = electropolished, SP = shot peened, BB = ball-burnished)
Figure 7. Residual stress-depth distribution after SP and BB in Ti-2.5Cu: (a) SP (0.20 mmA), (b) BB (HG6, 300 bar)
Figure 8. Pre-stress-depth distribution in Ti-2.5Cu

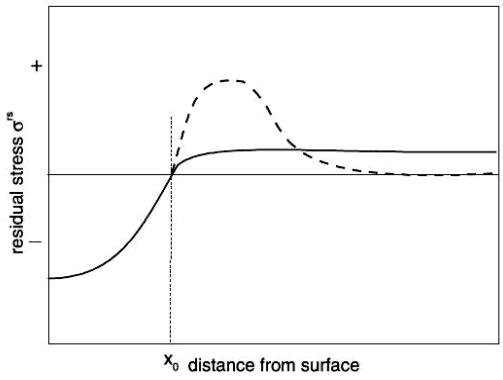

Figure 1. Schematic presentation of the residual stress-depth distribution which might be expected after mechanical treatments, x_o denotes the zero-crossing depth [5]

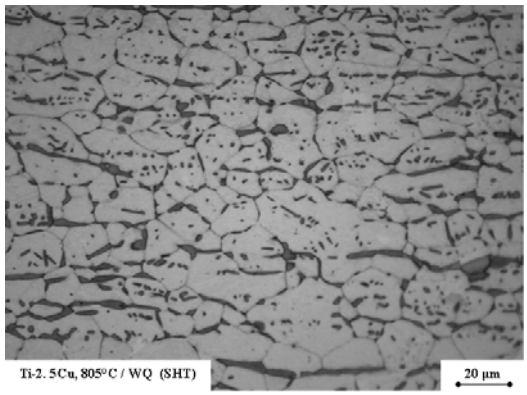

Figure 2. Microstructure of the Ti-2.5Cu alloy (SHT), average grain size ≈ 20 µm

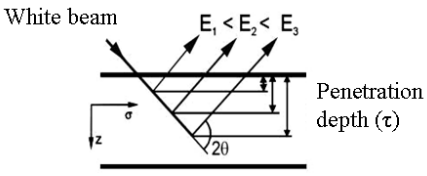

Fig. 3. Scheme showing a relation between energy and penetration depth

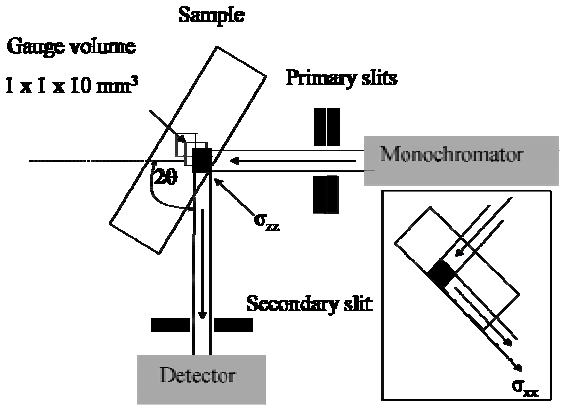

Fig. 4. Schematic set-up of the neutron scattering experiment at FRM-II

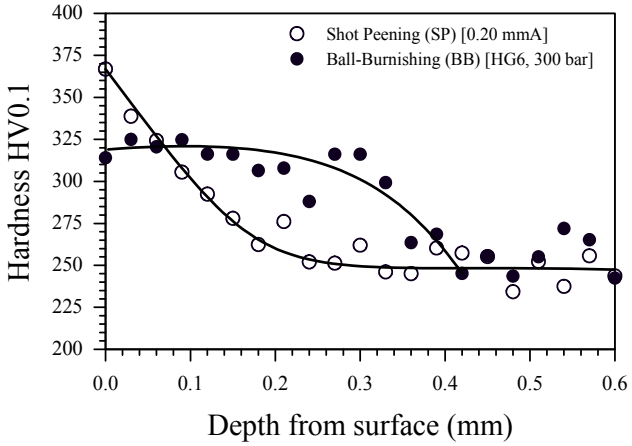

Figure 5. Microhardness-depth distribution of Ti-2.5Cu after SP and BB

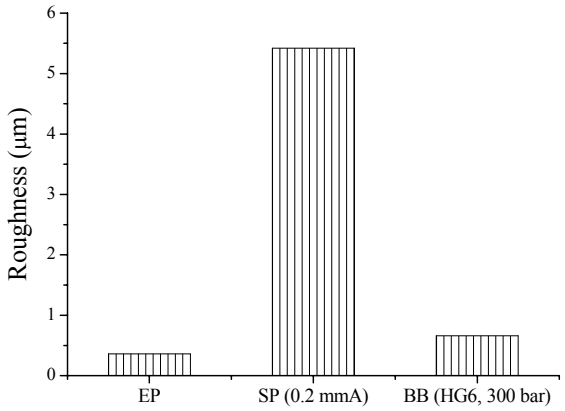

Fig. 6. Roughness values of the various surface treated conditions in Ti-2.5Cu (EP = electropolished, SP = shot peened, BB = ball-burnished)

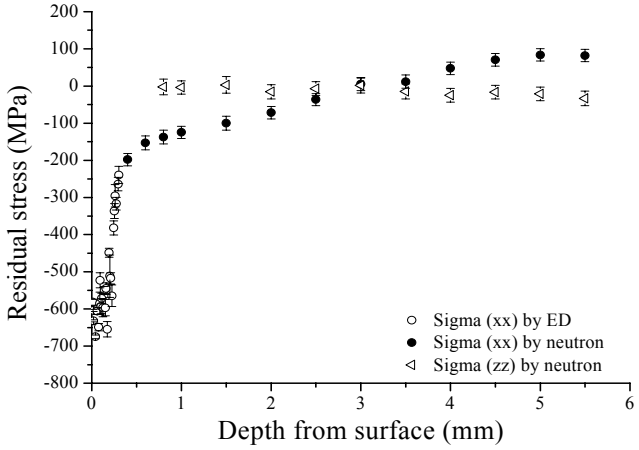

Fig. 7 a

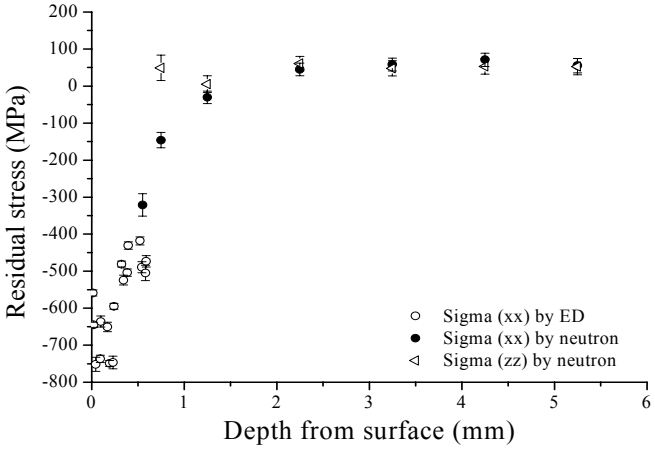

Fig. 7 b

Fig.7. Residual stress-depth distribution after SP and BB in Ti-2.5Cu:
(a) SP (0.20 mmA), (b) BB (HG6, 300 bar)

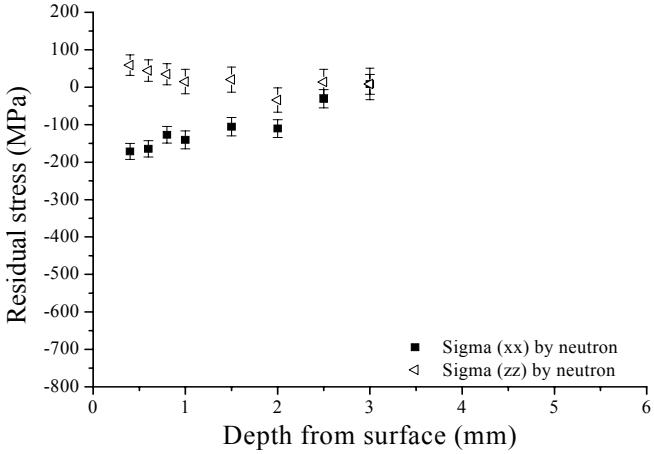

Fig. 8. Pre-stress-depth distribution in Ti-2.5Cu

Table 1. Tensile properties of Ti-2.5Cu (SHT)

E [GPa]	σ_y [MPa]	UTS [MPa]	e_u [%]	$\varepsilon_f = \ln (A_o/A_f)$
105	520	610	14	0.62

E = modulus of elasticity, σ_y = yield stress, UTS = ultimate tensile stress, e_u = elongation, ε_f = reduction

Table 2. Neutron diffractometer parameters

Wavelength	1.42 Å
Monochromator	Si (400)
Detector	PSD, 20 x 20 cm^2
Slit size	Primary Slit: 1 x 10 mm^2
	Secondary slit: 1 mm
Detector distance	1035 mm
2-Theta (hk.l)	97.1° (21.1) & 101.4° (11.4)

Table 3. Summarization of residual stress values after SP and BB

	RS close to surface		Maximum RS		Zero-crossing		Tensile RS		Improvement of HCF [%] [3]
	σ_{xx} [MPa]	τ [µm]	σ_{xx} [MPa]	τ [µm]	σ_{xx} [MPa]	τ [µm]	σ_{xx} [MPa]	τ [µm]	
SP	-582	14	**-687**	**92**	0	**3000**	100	Const.	**45**
BB	-559	14	**-750**	**194**	0	**1500**	50	Const.	**60**

σ_{xx} = residual stress, τ = depth, Const. = constant values, HCF = high cycle fatigue strength